Journal of Molecular Graphics and Modelling 28 (2010) 746–754

Contents lists available at ScienceDirect

Journal of Molecular Graphics and Modelling

journal homepage: www.elsevier.com/locate/JMGM

Molecular orbital model of the influence of interaction between O_2 and aluminosilicate sites on the triplet–singlet energy gap and reactivity

Yoana Pérez-Badell, Rachel Crespo-Otero, Enrique Méndez-Vega, Luis. A. Montero *

Laboratorio de Química Computacional y Teórica, Facultad de Química, Universidad de La Habana, calle Zapata s/n, 10400 Havana, Cuba

ARTICLE INFO

Article history:
Received 27 November 2009
Received in revised form 14 January 2010
Accepted 31 January 2010
Available online 6 February 2010

Keywords:
Aluminosilicate
Oxygen molecule
Computational modelation

ABSTRACT

The behavior of O_2 molecule in models of acid aluminosilicate sites on any kind of material was investigated using reliable QM *ab initio* calculations. The triplet–singlet energy gap of isolated O_2 was calculated at confident levels of theory with different basis sets as a reference. Models of aluminosilicate active sites interacting with oxygen in their singlet and triplet electronic states were considered for two kinds of O_2 arrangements. Geometry optimizations were performed on both non-corrected and corrected BSSE potential energy surfaces, realizing that good modeling of heavy atom–hydrogen interactions is sensitive to BSSE corrections during these processes. Energies were further evaluated at higher level of theory to test tendencies. Singlet oxygen appears more attractive to active aluminosilicate sites than those calculated with triplet oxygen, indicating a source of oxidative efficiency for designed nanostructures containing such molecular residues. It was clearly seen that aluminosilicate groups, appearing ubiquitously in several materials, could reduce the O_2 triplet–singlets energy gap by at least 10 kJ/mol. Some elegant features of oxygen interactions with such sites were further analyzed by means of the atoms in molecules (AIM) theory.

1. Introduction

Inorganic systems designed as catalysts on demand are part of the strategy of material sciences long ago [1]. On the other hand, catalysts in well designed nano-environments are very promising for most of the current necessities of human society as, for example, efficient solar conversion of carbon dioxide and water vapor to methane and other hydrocarbons using nitrogen-doped titanium nanotube arrays to replicate photosynthesis in any way [2]. The opposite action to facilitate oxidation is currently managed in many ways, and the role of singlet O_2, as a very active species is relevant for all techniques.

At present, theory and computations continue to play an important role in developing our understanding of O_2 and complexes of oxygen with other molecules, particularly with respect to phenomena that involve singlet oxygen [3]. O_2 molecule plays a key role in many natural life processes. Naturally occurring triplet oxygen plays an evident role for maintenance of life in the current geological stage of earth. On the other hand, the photochemistry, photobiology and photophysics of singlet molecular oxygen also affect our lives in a continuous and rather significant way. This molecule has applications in areas such as biomolecular degradation and photosensitized oxidations in material sciences [4]. In general, O_2 molecule has many properties related with energy transfer processes and chemical reactivity. For example, interaction of oxygen molecule and water is very important from the point of view of atmosphere, environment, weather and agriculture. There are theoretical reports related with this interaction [5,6]. When two oxygen atoms are bound, there are three closely energetically related electronic states: the triplet state ($^3\Sigma_g^-$) that become with the lowest energy and two higher singlet states ($^1\Delta_g$ and $^1\Sigma_g^+$). O_2 ($^1\Delta_g$) is a meta-stable species that is commonly called singlet oxygen [7].

On the other hand, most of the olefin oxidation mechanisms that occur in microporous materials as zeolites, imply the intervention of singlet O_2 [8]. Direct experimental proofs of the presence of singlet oxygen on this surface have been obtained [9]. These reactions are associated with significant applications in several fields, including organic synthesis. Photooxidations by oxygen molecules and subsequent olefins reactions on zeolites have been investigated by experimental papers [10–12] as well as those using *ab initio* and semiempirical electronic structure methods [13–17]. There are also very recent reports that the singlet oxygen participates in hydrocarbon reactions, in particular, in the formation of radical cations as active intermediates [18].

* Corresponding author. Tel.: +53 7 878 1263; fax: +53 7 873 5774.
E-mail addresses: lmc@fq.uh.cu, luis.montero@quimica.uh.cu, qct@infomed.sld.cu (Luis. A. Montero).

1093-3263/$ – see front matter © 2010 Elsevier Inc. All rights reserved.
doi:10.1016/j.jmgm.2010.01.012

O_2 adsorption is also widely used in industry. Experimental techniques and theoretical methods have been used to study the interactions of oxygen molecule [19–22]. Several reports of fundamental absorption data of O_2 in cation exchanged zeolites [22–25] and in H-form zeolites [26,27] have been published. Oxygen sorption on the pores of HY, H-ZSM-5 and H-MOR has been studied by FT-IR and used to determine which Brønsted acid sites are accessible to oxygen molecule [26,28,29]. O_2 has been used as a shift reagent to prove accessibility of cations and protons in zeolite by Liu et al. [26]. These papers report that oxygen can interact with surface hydroxyls of the supercage protons: the Brønsted acid and silanol protons. Oxygen molecule has been found to form 1:1 H-bonded complexes with the acidic OH groups [30].

In a recent study, interactions of O_2 and N_2 with extraframework cations of aluminosilicate materials were investigated using the B3LYP density functional by Mikosch et al. [31]. They concluded that the N_2 adsorption complexes with the extraframework cations are linear, while those with O_2 are bent regardless of the extraframework cations location. Alternatively, for a few configurations of the bulk nitrite sodalite–O_2 system, the triplet–singlet energy gap was calculated and it is reduced to a few kJ/mol. This result indicates a stabilization of singlet oxygen in this system [32]. O_2 adsorption in proton, sodium and copper exchanged chabazite has been studied using periodic and cluster approaches by us, in a recent publication [33]. In our paper, O_2–HCHA adsorption complexes present an O_2 bent coordination and the adsorption energies are due to dispersion. We also report that only the highest singlet oxygen interaction is more stabilized in HCHA than the triplet state.

The discussion of interaction processes involving singlet and ground state oxygen is required to achieve a complete understanding of the energy transfer mechanism of the photochemical reactions that occur in aluminosilicate materials. Transitions between triplet and singlet states are forbidden by Wigner's spin selection rule; it means that they show a small probability in normal conditions. One open question is the influence of the environment in the stabilization of singlet electronic state of O_2 molecule. The effect of silicate and aluminosilicate clusters on the triplet–singlet gap is evaluated in this study. For this reason, complexes with O_2 ($^3\Sigma_g^-$), O_2 ($^1\Delta_g$) and O_2 ($^1\Sigma_g^+$) were modeled.

The aim of the present work is then to investigate the behavior of O_2 molecule (at triplet and singlet electronic states) in silicate and aluminosilicate environment. Starting with a short presentation of O_2 triplet–singlet gap calculated at high levels of theory and different basis sets, we tested the performance of the employed level of theory. After that, the gap was estimated in the presence of silicate and aluminosilicate environment. In these cases, calculations were performed at MP2/6-311G(d,p) and MP2/6-311++G(2d,2p) levels of theory. A detailed study of the O_2–silicate and O_2–aluminosilicate complexes was carried out at the previous level and exploring BSSE-uncorrected PES and BSSE-corrected PES. Atoms in molecules (AIM) theory has also been used to study and characterize these kinds of interactions [34].

2. Methods and models

We recognize that from a theoretical and computational perspective, this simple system has limitations and difficulties because O_2 and O_2-complexes are open-shell systems in which valence orbitals are not completely filled. Nowadays, the open-shell problem is at the head of modern research in quantum chemistry.

Some papers report that the description of singlet oxygen molecule could be afforded as a multi-configurational problem using the multireference single and double excitation configuration interaction (MRSDCI) method [35]. However, we obtain that O_2 calculations could be also afforded using MP2 level as we demonstrate here. Literature also reports calculation of polar water–O_2 complexes [5,6]. On the other hand, size consistency is absent in configuration interaction and it plays an important role when molecular interactions and multiple body pre-reactive states are calculated.

Firstly, we calculated the O_2 triplet–singlet gap using B3LYP, MP2, CCSD(t) and CISD with different combinations of basis sets. After that, results are compared with literature in order to validate our choice. Natural atomic and bond orbital population analysis were performed to test the correct electron distribution after the single determinant procedures were used in this paper. There were not relevant cases where NBO analyses indicated an incorrect electron occupation.

The $^1\Delta_gO_2$ complexes have been computed using the UB3LYP unrestricted formalism. This formalism suffers from spin contamination. Thus, the obtained energy values for all $^1\Delta_gO_2$ containing systems have been corrected by Yamaguchi et al.'s projection [36].

On the other hand, in order to obtain an accurate representation of intermolecular complexes, MP2 and Kohn–Sham's DFT are the most widely used methods. We decided to use MP2 [37] due to the unpredictable behavior of some KS-DFT functionals in the case of very weak intermolecular complexes [38,39]. The selection of basis sets is a difficult point. In this study, the polarized 6-311G(d,p) basis set was used for all atoms. This basis is of triple-zeta quality and sufficiently good to include the polarization of electron density due to hydrogen bonds. Its performance is also good at MP2 level [40].

In addition, BSSE is an important source of error in quantum mechanical calculations of intermolecular complexes, mostly when interactions are weak of unknown. This error must be removed in each optimization step, if we want to obtain qualitative and quantitative results [41]. In this study, the BSSEs were calculated using the counterpoise procedure (CP) proposed by Boys and Bernardi [42] and the influence of this problem on geometries was also analyzed. Interaction energies were calculated according to the supermolecular approach and without BSSE correction. After that, CP was used to correct both the optimized geometries and the interaction energies. Single-point calculations with MP2/6-311++g (2d,2p) have been also carried out using the optimized structures obtained with the MP2/6-311G(d,p) level of theory. This basis set has a good performance for other weak complexes of open-shell systems previously studied by us [39]. Full structure optimizations of the clusters were performed without geometry restriction or fixed coordinates. The contribution of the relaxation of the aluminosilicate geometry during the optimization process is not significant in the results.

In order to test the influence of the electrostatic field, in the singlet–triplet O_2 energy gap, calculations at MP2/6-311G(d,p) level by the simple Onsager [43] model were done. In this model, a dipole in the molecule induces a dipole in the medium and the electric field applied by the solvent dipole interacts with the molecular dipole. We use the geometries of the biggest aluminosilicate–O_2 complex in gas phase (calculated at MP2/6-311G(d,p) level of theory). The solute was located in a spherical cavity of 4.44 Å radius within the solvent field. This radius was calculated as the involved in the volume inside a contour of 0.001 electrons/bohr^3 density of solute molecule in the triplet state. The simplicity of this model allows testing the effect of dielectric constant of the medium without the influence of the shape of the solvent included in more sophisticated models like PCM [44]. Dielectric constants from 1 up to 80 were considered.

Unrestricted approach was used for open-shell species. All calculations were performed using Gaussian 98 [45] and Gaussian 03 [46] programs. PLUTO representations were obtained with ORTEP-3 for Windows [47].

2.1. Silicate and aluminosilicate models

At this moment, the most accurate quantum calculation of the whole zeolite cell is limited by computer resources. We selected relatively small cluster models in order to include electron correlation and performing geometry optimization at reasonable computer times. They appear to be appropriate for the calculation of association properties in previous [30] and even very recent works [48–50]. Obviously, the cavity can affect the diffusion and accommodation of adsorbed molecules and this could be a shortcoming of this model. However, O_2 is a small molecule and consequently shows no large steric hindering in zeolite cavities. On the other hand, Kyrlidis et al. [51] demonstrated that Madelung fields have no effect on the structural properties of small clusters in the acid site. Comparison between quantum-chemical calculations on silicate and aluminosilicate clusters and force field calculations on extended systems shows that the relative energy content of neutral-framework is determined by the smallest substructure energies. These results justify the use of small clusters for accurate theoretical studies [52].

Silanol groups on amorphous silica and in H-form zeolites have been reported to form H-bondings [28] that represent terminal hydroxyls at the surfaces or defect sites. Therefore, in order to study the nature of terminal silica hydroxyls, the silanol models were used. Silanol [H_3SiOH], the simplest molecular model of tetrahedral silicon, and orthosilicic acid [$(OH)_3SiOH$] were studied. The latter includes a set of OH neighbors. Their stoichiometries are H_4SiO and H_4SiO_4, respectively.

Brønsted sites were represented using $H_3Si(OH)AlH_3$ and $H_3SiOAl(OH)_2(OH)SiH_3$ models. These cluster models have been previously used in the literature to represent acid sites [53]. In the model $H_3SiOAl(OH)_2(OH)SiH_3$, two hydrogen atoms as well as two SiH_3 are attached to the central AlO_4 tetrahedron. This model retains one and half coordination spheres of the central aluminum atom. Their stoichiometries are H_7SiAlO and $H_9Si_2AlO_4$, respectively. The optimized models are shown in Fig. 1. Two types of interaction of O_2 molecule were considered: linear and the π electron cloud interaction.

Atoms in molecules (AIM) theory is a very useful tool to analyze H-bonds (HBs) and van der Waals (vdWs) complexes. Interactions in silicate and aluminosilicate clusters have been previously studied employing AIM theory [48]. The MP2 electron densities of the complexes in their singlet and triplet states were analyzed using the AIM2000 programs [54]. Critical points were detected and the contour plots of the electron density were visualized.

3. Results and discussion

3.1. Calculation of isolated O_2 gap using different methods and basis sets

In order to evaluate the performance of MP2 level in the description of O_2 molecule complexes, the isolated O_2 gap was calculated using different methods and basis sets (Table 1).

All calculated MP2 singlet–triplet gaps are in agreement with the experimental value. However, the best agreement with experimental gap is obtained with the MRCI/[5s4p(3 + 1)d 2f 1g] + (sp) level [35]. Fois et al.'s [32] reports that obtained using DFT and Hartree–Fock approximation with a triple-zeta plus polarization basis set are obtained. MP2 method predicts very well the triplet–singlet gap.

3.2. Calculation of O_2 gap in aluminosilicate environment

The purpose is to verify if the energy is perturbed when the oxygen interacts with these environments. The results are shown in Table 2. In all cases the energy is positive because we considered the triplet state as a reference. We have analyzed the variation of the relative stabilities of $^3\Sigma_g^-$, $^1\Delta_g$ and $^1\Sigma_g^+$ O_2 electronic states due to the effect of the zeolite framework

The effect of the aluminosilicate cluster in the stabilization of O_2 singlet states is important. Singlet state is stabilized in this media

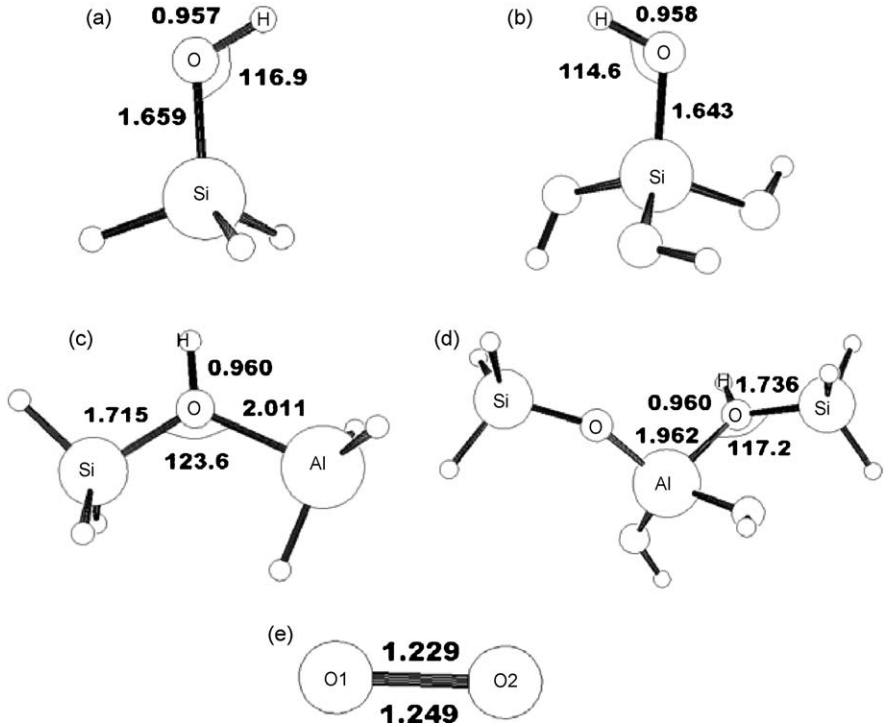

Fig. 1. Optimized geometries of molecular models at MP2/6-311G(d,p) level. Terminal OH group of silica (a and b), bridging OH group of zeolites (c and d) and oxygen molecule (e, roman: $^1\Sigma_g^+$; italic: $^3\Sigma_g^-$).

Table 1
Isolated singlet–triplet oxygen gap calculated by different methods (in kJ/mol).

Methods	$^3O_2$–$^1\Delta_gO_2$[a]	$^3O_2$–$^1\Sigma_g^+O_2$
MP2/6-311G(d,p)	98.0	130.2
MP2/6-311++G(2d,2p)	95.5	125.4
CCSD(t)/6-311++G(2d,2p)	83.2	126.9
CISD/6-311++G(2d,2p)	112.5	157.0
MRCI/[5s4p(3+1)d 2f 1g]+(sp)[b]	94.2	–
Experiment[c]	94.8	157.0

[a] Energy difference after Yamaguchi et al.'s spin projection.
[b] Ref. [35].
[c] T.G. Slanger, P.C. Cosby, J. Phys. Chem. 92 (1988) 267.

with respect to the gas phase. In the case of $^1\Sigma_g^+$ O_2 electronic state in largest model, the stabilization is of around 13.8 kJ/mol (using corrected energies at the highest level of theory: MP2/6-311++G(2d,2p)). Fois et al. [32] studied the intracage oxidation in sodalite unit by means of the blue moon ensemble and Car Parrinello MD combined methods. Their results also suggest that interactions in the cage reduce the O_2 triplet–singlet energy gap.

$^1\Sigma_g^+$ O_2 adsorbs in through the similar coordination mode than the other two more stable states. Nevertheless, all calculated $^1\Sigma_g^+$ O_2 complexes present shorter OH···O_2 distances. Therefore, the energy gap between the $^3\Sigma_g^-$ and the $^1\Sigma_g^+$ electronic states decreases 13.8 kJ mol^{-1} inside the largest model.

In the most relevant case (aluminosilicate environment), the effect of the electrostatic field on the singlet–triplet gap was also explored employing the simple Onsager model. The most stable complexes corresponding to the largest model were used. The geometries employed were the obtained on corrected BSSE surfaces. The singlet–triplet gap behavior with dielectric constant was evaluated in media of different dielectric constants. Fig. 2 plots the predicted energy difference by Onsager method and solvent environment dielectric constant (ε = 1 corresponds to the complex without perturbation of dielectric field, and thus this value is different from the obtained with the O_2 in gas phase). According to this model, an increase in the dielectric constant produces a larger gap up to reaching a limit (about 120 kJ/mol). Therefore, the triplet state is stabilized in polar media with respect to the singlet one. The energy gap obtained for O_2 in gas phase at this level is 130 kJ/mol, which is larger than the obtained limit value. The effect of dielectric constant does not increase the energy gap more than the value in gas phase, and the zeolite field decreases the gap with respect to the gas phase.

In general, aluminosilicates materials have a small dielectric constant (<10). These results are also congruent with the well known fact that zeolites are a suitable medium for oxidation reactions.

3.3. Terminal silica hydroxyl models [SiOH] and their interaction with triplet and singlet O_2 molecule

The acidic hydroxyls of amorphous silica are mimicked by the minimal cluster H_3SiOH and $(OH)_3SiOH$. Optimized geometries of both molecules are shown in Fig. 1. The geometries are in concordance with the literature reports [30].

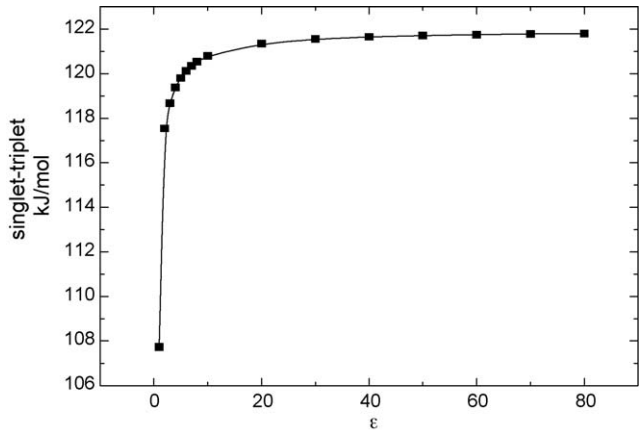

Fig. 2. $^1\Sigma_g^+O_2$ – triplet gap versus dielectric constant calculated according Onsager model. (This is the gap corresponding to the $H_{11}Si_2AlO_4$–O_2 molecule complexes.)

Figs. 3 and 4 show geometrical relevant parameters of the interaction on CP-corrected and uncorrected PESs for each orientation (linear and T-shape). For triplet complexes bonding via T-shape geometry does not yield a bounded structure. In the bonding via linear, we can see that the O_2 molecule was not located on the straight line given the O–H bond of model.

There are not appreciable changes in the geometries of complexes respect to the geometries of the isolated molecules. Singlet oxygen shows the most strong interaction with the clusters. This is obtained in corrected or uncorrected PES.

As expected, an increase in all intermolecular distances for CP-corrected PES is obtained. These results differ around 0.1 Å from the values obtained on CP-uncorrected PESs for all complexes. The most important effect of BSSE in the geometries is related with variation of intermolecular angles. The φ_{O-H-O1} and $\varphi_{H-O1-O2}$ angles determine the orientation between both molecules. They change more than eight degrees after the optimization on corrected BSSE PESs. The obtained complexes are near-to-linearity, showing that the use of functions from the distant oxygen in the variational optimization process decreases the angle artificially. This behavior shows the importance of carrying out the optimization in a BSSEs free PES.

All the arrangements for oxygen are of attractive nature and lead to formation of adsorption complexes. The association energies computed at the MP2/6-311G(d,p) level are shown in Table 3. The interaction energies of singlet complexes are smaller than those of triplet ones, due to the higher affinity of the highest singlet state in comparison with triplet one.

The optimized geometries for adsorbed $^1\Delta_gO_2$ molecule are very close to that obtained for $^3\Sigma_g^-$ O_2 as illustrated by the fact that O_2 always present the similar adsorption energies to that of the fundamental state and that the OH···O_2 bond distances and

Table 2
Singlet–triplet oxygen gap in aluminosilicate environment (in kJ/mol)[a].

	Isolated $^3O_2$–$^1\Delta_gO_2$ gap[b]	$^3O_2$–$^1\Delta_gO_2$ gap in aluminosilicate environment[c]	Isolated $^3O_2$–$^1\Sigma_g^+O_2$ gap[b]	$^3O_2$–$^1\Sigma_g^+O_2$ gap in aluminosilicate environment[c]
Uncorrected PES's MP2/6-311G(d,p)	98.0	92.0	130.2	115.6
Corrected PES's MP2/6-311G(d,p)	98.0	97.0	130.2	120.5
Corrected PES's MP2/6-311++G(2d,2p)//MP2/6-311G(d,p)	95.5	94.5	125.5	111.7

[a] Energy difference after Yamaguchi et al.'s spin projection.
[b] Isolated O_2 gap as: $E(^1O_2) - E(^3O_2)$.
[c] O_2 in aluminosilicate environment gap as: $E(H_{10}Si_2AlO_4H\cdots{}^1O_2) - E(H_{10}Si_2AlO_4H\cdots{}^3O_2)$.

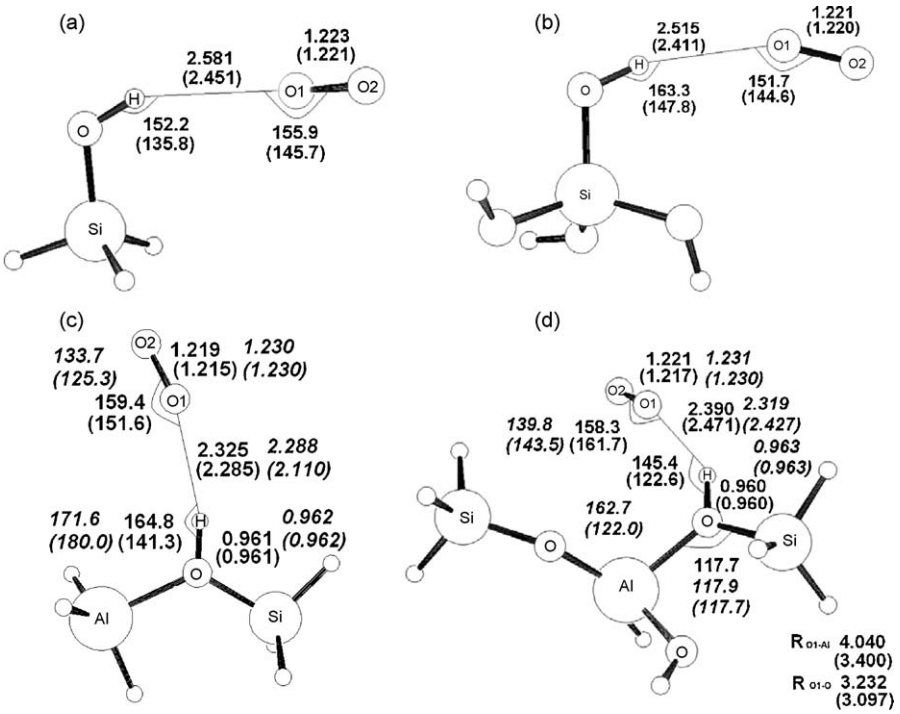

Fig. 3. Geometrical data for the optimized stationary points of complexes with $^3O_2$ and $^1\Delta_gO_2$ (cursive) in CP corrected and CP uncorrected (in parentheses) at MP2/6-311G(d,p) level.

OH···O–O angles are closed to those reported for $^3\Sigma_g^-O_2$ complexes. This is associated with a no significant variation in the triplet–singlet relative energies.

BSSEs are important in corrected and uncorrected PESs. When the counterpoise correction is applied as a single point, the obtained BSSE in the fixed geometries are large and the energy balance produces less stable complexes (the CP correction is about more than 50% of the interaction energy, showing again that it cannot be ignored). The BSSE obtained in the corrected PES is always smaller than the BSSE in uncorrected ones. However, the values of BSSEs are still considerable in corrected geometries (see Table 4). The large values of BSSE are commonly found in MP2 calculations, and our significant BSSE contaminations are not surprising [55].

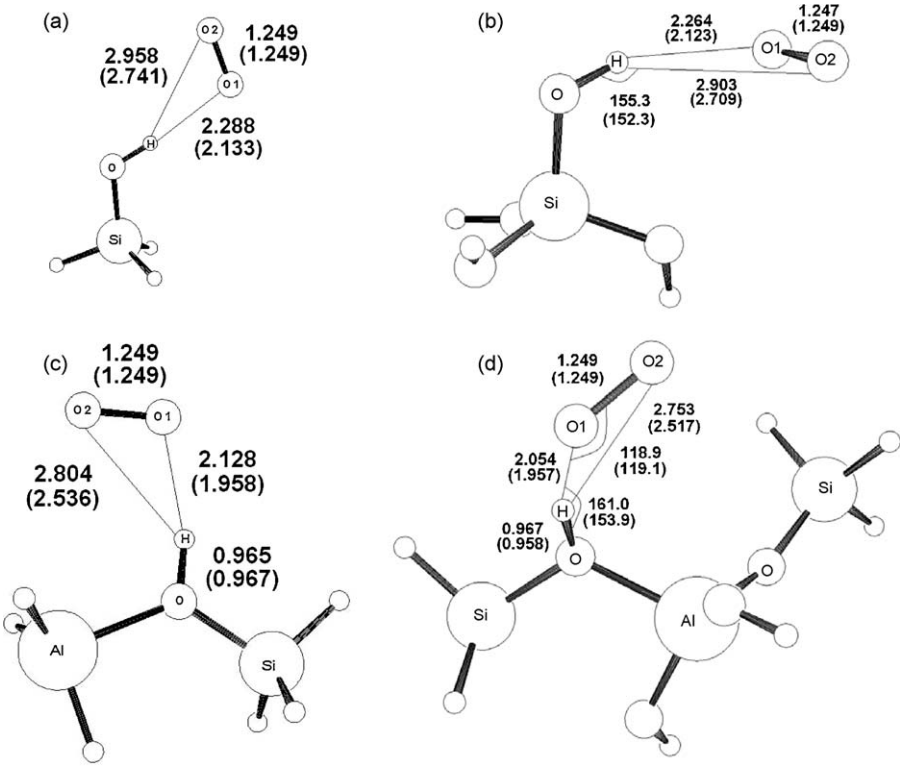

Fig. 4. Geometrical data for the optimized stationary points of complexes with $^1\Sigma_g^+O_2$ in CP corrected and CP uncorrected (in parentheses) at MP2/6-311G(d,p) level.

Table 3
Association energies (kJ/mol) of the complexes between silica models and O_2 molecule at MP2/6-311g(d,p) level.

Complexes	E_{uncorr}[a]	E_{corr}(CP)[b]	$E_{MP2/6-311++g(2d,2p)}$(CP)[c]
$^3O_2\cdots H_4SiO$	−6.04	−2.30	−2.08
$^3O_2\cdots H_4SiO_4$	−6.96	−3.24	−2.32
$^1\Delta_gO_2\cdots H_4SiO$	−6.36	−2.52	−2.12
$^1\Delta_gO_2\cdots H_4SiO_4$	−4.25	−2.04	−1.95
$^1\Sigma_g^+O_2\cdots H_4SiO$	−11.21	−6.29	−6.57
$^1\Sigma_g^+O_2\cdots H_4SiO_4$	−16.01	−8.58	−9.37

[a] Energy of stabilization as: $E(\text{Model}\cdots{}^{1(3)}O_2) - E(\text{Model}) - E({}^{1(3)}O_2)$ contaminated by BSSE.
[b] Counterpoise corrected interaction energy at the geometry found for the BSSE-corrected PES.
[c] Counterpoise corrected interaction energy at MP2/6-311++G(2d,2p)//MP2/6-311G(d,p).

Table 5
Association energies (kJ/mol) of the complexes between aluminosilicate models and O_2 molecule at MP2/6-311g(d,p) level.

Complexes	E_{uncorr}[a]	E_{corr}(CP)[b]	$E_{MP2/6-311++g(2d,2p)}$(CP)[c]
$^3O_2\cdots H_7SiAlO$	−8.37	−4.16	−3.31
$^3O_2\cdots H_{11}Si_2AlO_4$	−11.03	−4.18	−4.30
$^1\Delta_gO_2\cdots H_7SiAlO$	−9.02	−4.84	−4.14
$^1\Delta_gO_2\cdots H_{11}Si_2AlO_4$	−11.68	−4.70	−4.61
$^1\Sigma_g^+O_2\cdots H_7SiAlO$	−20.59	−11.87	−12.72
$^1\Sigma_g^+O_2\cdots H_{11}Si_2AlO_4$	−25.53	−13.87	−17.92

[a] Energy of stabilization as: $E(\text{Model}\cdots{}^{1(3)}O_2) - E(\text{Model}) - E({}^{1(3)}O_2)$ contaminated by BSSE.
[b] Counterpoise corrected interaction energy at the geometry found for the BSSE-corrected PES.
[c] Counterpoise corrected interaction energy at MP2/6-311++G(2d,2p)//MP2/6-311G(d,p).

As can be seen, there is an improvement in the energy when the single-point calculations are done by MP2/6-311++G(2d,2p)//MP2/6-311G(d,p) level. In all cases the BSSE is reduced. The singlet complexes become more stable and triplet complexes less attractive, in comparison with MP2/6-311G(d,p) calculations.

3.4. Brønsted site models [Si(OH)Al] and their interaction with singlet and triplet O_2 molecule

Acidic hydroxyls of aluminosilicate materials are mimicked by the minimal cluster $H_3Si(OH)AlH_3$ and $H_3SiOAl(OH)_2(OH)SiH_3$. Optimized geometries of the two molecules are shown in Fig. 1.

In both models, the predicted aluminum oxygen bond length is larger than the reported by experimental results, and it is even larger than the silicon–oxygen bond length. In $H_3SiOAl(OH)_2(OH)$-SiH_3 model, are two different Si–O–Al bridges. As can be seen in Fig. 1, the Si–O(H)–Al bond angle is smaller than the Si–O–Al one. It indicates that the bridging oxygen is screening the electrostatic repulsion between the proton and the aluminum atom. It is in concordance with the reported results. It shows the relative flexibility of this framework.

The most important optimized geometry parameters of the complexes for Brønsted sites with O_2 in CP-uncorrected and -corrected PESs are shown in Figs. 3 and 4. Calculations with the $H_3Si(OH)AlH_3$ model yielded bound complexes with O_2 in both states. However, interaction via linear with the second $^1O_2$ did not yield a bound stationary structure like in the silicate clusters.

The distance in linear arrangement is about 2.29 Å for triplet O_2 and through via π electron cloud for about 2.52 Å. When both configurations can be obtained, the linear is the strongest. The $H_3Si(OH)AlH_3$-triplet oxygen (T-shape geometry) complex gives a chance to this structure to exist during a process that could involve these interactions (Fig. 2). However, it is only a chance and not a preferred structure, regarding the results of this paper.

The related stabilization energies indicate that a weak interaction has occurred. The association has little effect on the geometry of the model and the O1–O2 distance is not significantly affected. Wakabayashi et al. [28,29] report that the interaction of O_2 with the bridging hydroxyl groups would occur through O_2 in preferably linear orientation and it is rather weak. At the same time, the frequency of the ν(O–O) is not significantly changed after the association.

In the case of linear bonding (Fig. 3), we can also show that the O_2 molecule was not on the straight line with the O–H bond of the acid site. These findings are in agreement with the DFT results reported by Mikosch et al. [31] who states that O_2 forms a bent structure.

The effect of BSSE in geometries is really significant for the T-shape complexes changing the intermolecular distances around 0.3 Å. For linear complexes, the effect of BSSE in intermolecular distances is not considerable. However, again the corrected BSSE complexes are near-to-linearity due to the artificial use of the O partner orbitals in uncorrected PES optimizations. As expected, CP-corrected intermolecular distances are larger than CP-uncorrected PES distances.

An important property of the adsorption complexes is their interaction energy. This kind of energy gives a measure of the degree of binding in the formation of adsorption complexes. The interaction energies for this model are shown in Table 5. The absolute binding energies are larger in the case of Brønsted acid sites than in silanol sites. In the CP-uncorrected cases, for both orientations, R (OH–O_2) distances appear larger for triplet than singlet complexes.

In conclusion, zeolites models interact equally with $^3\Sigma_gO_2$ and $^1\Delta_gO_2$ leading to a no significant alteration of the triplet $^3\Sigma_g \rightarrow {}^1\Delta_g$ gap after adsorption. The interaction with the most energetic $^1\Sigma_gO_2$ is slightly stronger reducing the energy gap with respect to the fundamental state between 10 and 15 kJ mol^{-1}.

In comparison with MP2/6-311++G(2d,2p), the BSSE error is reduced. Obviously, in all cases, CP-corrected geometries give a reduced BSSE (Table 6).

Experimentally, the degree of interaction of O_2 with aluminosilicate materials can be estimated from changes in the OH valence vibrational frequencies. The perturbation suffered by the O_2

Table 4
Total defect of energy originated due to the basis set superposition error at the geometry of silica models–O_2 complexes found for the uncorrected PES and corrected PES (in kJ/mol).

Complexes	$BSSE_{uncorrPES}$[a]	$BSSE_{corrPES}$[b]	$BSSE_{corrPESMP2/6-311++G(2d,2p)}$[c]
$^3O_2\cdots H_4SiO$	4.78	2.72	1.89
$^3O_2\cdots H_4SiO_4$	5.86	2.98	2.43
$^1\Delta_gO_2\cdots H_4SiO$	5.14	4.65	2.96
$^1\Delta_gO_2\cdots H_4SiO_4$	8.70	5.94	4.26
$^1\Sigma_g^+O_2\cdots H_4SiO$	4.94	4.39	2.91
$^1\Sigma_g^+O_2\cdots H_4SiO_4$	8.71	5.96	4.34

[a] The basis set superposition error at the geometry found for the uncorrected PES.
[b] The basis set superposition error at the geometry found for the corrected PES.
[c] The basis set superposition error at MP2/6-311++G(2d,2p)//MP2/6-311G(d,p).

Table 6
Total defect of energy originated due to the basis set superposition error at the geometry of aluminosilicate models–O_2 complexes found for the uncorrected PES and corrected PES (in kJ/mol).

Complexes	$BSSE_{uncorrPES}$[a]	$BSSE_{corrPES}$[b]	$BSSE_{corrPESMP2/6-311++G(2d,2p)}$[c]
$^3O_2\cdots H_7SiAlO$	5.15	3.09	2.64
$^3O_2\cdots H_{11}Si_2AlO_4$	9.29	4.50	3.68
$^1\Delta_gO_2\cdots H_7SiAlO$	4.98	3.77	2.91
$^1\Delta_gO_2\cdots H_{11}Si_2AlO_4$	9.68	4.37	3.61
$^1\Sigma_g^+O_2\cdots H_7SiAlO$	7.57	7.29	4.31
$^1\Sigma_g^+O_2\cdots H_{11}Si_2AlO_4$	13.43	9.49	6.59

[a] The basis set superposition error at the geometry found for the uncorrected PES.
[b] The basis set superposition error at the geometry found for the corrected PES.
[c] The basis set superposition error at MP2/6-311++G(2d,2p)//MP2/6-311G(d,p).

Table 7
Selected MP2/6-311G(d,p) harmonic frequencies for the isolated molecules and adducts (Si–O(H)–Al···$^3O_2$) with linear orientation in comparison with the experimental frequencies (in cm^{-1}).

Mode	$H_{11}Si_2AlO_4$	H-ZSM5[a]	H-MOR[b]
ν(O–H) free	3726	3616	3610
ν(O–H) complex	3731	3621	3616
$\Delta\nu$(O–H)	+5	+5	+6

[a] Ref. [28].
[b] Ref. [29].

molecule breaks the local symmetry and causes a red shift of such bands. It could be understood as a measure of the strength of interaction. A small change in frequency, suggests that O_2 weakly interacts with the OH group. A perturbation of the acidic OH band is interpreted as a formation of an H-bonded complex between the acidic OH group and the adsorbate.

The harmonic stretching data of the biggest complex are given in Table 7. Theoretical frequencies with respect to the isolated model and the corresponding experimental frequency of the triplet oxygen state adsorbed on H-ZSM5 and H-MOR are compared. The results are in concordance with the experiment, showing that our model reproduces qualitatively the behavior of these systems. The stretching frequency changes only a few amounts of cm^{-1}.

3.5. How does the multiplicity of O_2 affect the interaction with silicate and aluminosilicate models? An AIM study

In this part, the study was developed with triplet O_2 and $^1\Sigma_g^+$ O_2 sates, because the $^1\Sigma_g^+$ O_2 stabilization is larger than the singlet $^1\Delta_g$ one.

The topological features of the interactions calculated at critical points are summarized in Table 8. In all cases, there is a *bcp* between one oxygen atom of O_2 and the hydrogen atom of hydroxyl group which belongs to the cluster model (O–H···O). These O–H···O interactions are the responsible of the stabilization of the complexes in the triplet and singlet states. The small electron densities (ρ) and the positive value of $\bigtriangledown^2\rho$ at the *bcp*s are characteristics of weak interactions. Electron densities $\rho(bcp)$s are slightly smaller than the previously reported for O–H···O interactions in a group of $H_3SiOH.O$ acceptor intermolecular complexes studied by Beckmann et al. [48]. All of these interactions can be classified as closed-shell interactions; the depletion of electron density in the *bp* produces a concentration of electron density in the perpendicular directions and $|\lambda_1|/\lambda_3 < 1$.

The stabilization energies of complexes with O_2 singlet are larger than the obtained for triplet state. For the complexes in singlet state, the electron densities are at least the double of the value than in the triplet state. In spite of the similar features of HBs and vdWs molecular interactions, the magnitude of electron density and $\bigtriangledown^2\rho$ in typical HB and vdWs interactions are different. Typical HBs have larger electron densities and$\bigtriangledown^2\rho$ than the obtained in vdW complexes. Bader reports a $\rho(bcp)$ of 0.0198 and $\bigtriangledown^2\rho$ of 0.0623, for the interaction O–H···O in water dimer, a typical HB. For a vdW complex, Ne-HF, electron density is 0.0099 and $\bigtriangledown^2\rho$ = 0.0484 [56]. Although, the classification in HBs and vdW is controversial and many criteria can be established, the aluminosilicate···O_2 complexes at singlet state behaves similar to typical HBs and the complexes with triplet oxygen are more similar to typical vdW. On the other hand, the values of the $|V(r)|/G(r)$ ratio are slightly larger for the singlet than for the triplet state. Both facts are in accordance with the larger stabilization

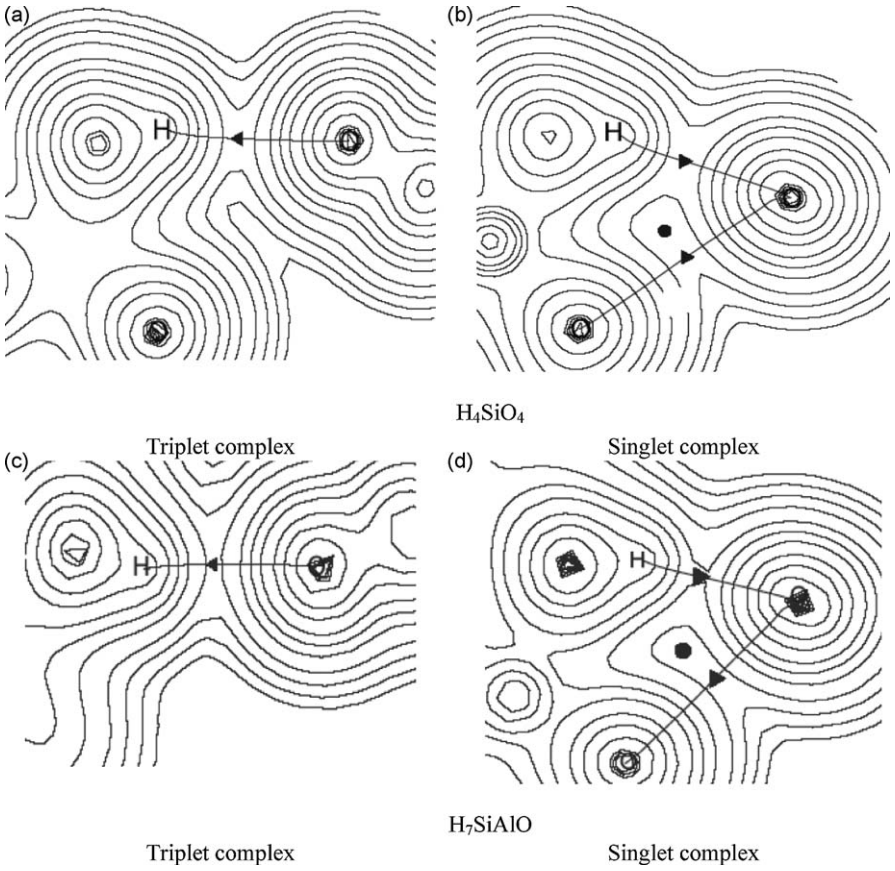

Fig. 5. Contour plot of the electron density of the $^1\Sigma_g^+O_2$ and triplet complexes calculated at the MP2/6-311G(d,p) level in the plane formed by the hydrogen atom of the hydroxyl group of zeolite model and oxygen atom of O_2 molecule, showing the bond paths. The contours increase in value in the order 2×10^n, 4×10^n, 8×10^n with n beginning at −3 and increasing by unity. (The outer contour is 0.001 au.) The *bcp*s are marked with triangles and the *rcp* with a dot.

Table 8
Bond critical point properties (in au) for singlet and triplet complexes by AIM theory.

		$\rho(bcp)$	$\nabla^2\rho(bcp)$	$G(bcp)$	$V(bcp)$	$\lvert V(bcp)\rvert/G(bcp)$
Singlet complexes						
H_4SiO	O–H···O	0.0112	0.0395	0.0085	−0.0071	0.8388
H_4SiO_4	O–H···O	0.0122	0.0428	0.0095	−0.0083	0.8734
	O···O	0.0045	0.0192	0.0041	−0.0034	0.8253
	rcp (0.44 Å)[a]	0.0041	0.0199	0.0040	−0.0031	0.7689
H_7SiAlO	O–H···O	0.0157	0.0569	0.0125	−0.0107	0.8585
	Al···O	0.0012	0.0049	0.0009	−0.0006	0.6506
	rcp (0.14 Å)[a]	0.0012	0.0054	0.0010	−0.0006	0.6464
$H_{11}Si_2AlO_4$	O–H···O	0.0185	0.0676	0.0151	−0.0133	0.8807
	O···O	0.0060	0.0241	0.0053	−0.0045	0.8575
	rcp (0.56 Å)[a]	0.0049	0.0236	0.0049	−0.0039	0.8013
Triplet complexes						
H_4SiO	O–H···O	0.0046	0.0189	0.0039	−0.0031	0.7839
H_4SiO_4	O–H···O	0.0051	0.0207	0.0042	−0.0033	0.7772
H_7SiAlO						
Linear	O–H···O	0.0072	0.0318	0.0062	−0.0045	0.7245
T-shape		0.0025	0.0109	0.0022	−0.0016	0.7252
$H_{11}Si_2AlO_4$	O–H···O	0.0066	0.0286	0.0058	−0.0044	0.7595
	Si–H···O	0.0005	0.0024	0.0004	−0.0002	0.4853
	rcp (0.32 Å)[a]	0.0004	0.0025	0.0004	−0.0002	0.4749

[a] Distance of the *rcp* to the previous *bcp*.

energy of the singlet state with respect to the triplet ones. The increasing of the model increases the electron density in the *bcp* and stabilizes the complexes.

In the case of H_7SiAlO complex in triplet state, there are two geometries, the linear and the T-shape complexes. The larger stability of the linear form could be also associated with the larger electron density in the O–H···O *bcp* (Table 8).

For the singlet state in the H_4SiO_4 and $H_{11}Si_2AlO_4$ models, appears a second interaction, the O···O, between one of the oxygen atoms of O_2 and one of the oxygen atoms belongs to the cluster. Similar O···O interactions have been reported for ice and they can be also classified also as closed-shell interactions [57]. These are weaker than the O–H···O as their values of electron densities shown (Table 8). Fig. 5 shows the relief map of the topology of electron density in the triplet and singlet states, the interactions O–H···O and O···O generate a cyclic structure with a corresponding *rcp*. The distances between *rcp* and O···O *bcp* are 0.44 and 0.56 Å.

Other weaker interactions appeared in these systems: Al···O and Si–H···O. The Al···O interaction has a very small electron density in the *bcp*. A *rcp* is localized only at 0.14 Å to the Al···O *bcp*, which shares essentially the same value of ρ and they are very close to annihilation, adding some instability to this intermolecular complex. It can be found the Si–H···O interaction in the $H_{11}Si_2AlO_4$ model. According to their electron densities, this interaction (Si–H···O) is the weakest, appearing a *rcp* at 0.32 Å, they can annihilate each other with a subsequence change in the topology.

4. Conclusions

The behavior of singlet and triplet O_2 molecule on polar environment was investigated by theoretical *ab initio* MP2 methods. The adsorption of $^1\Delta_g$ and $^1\Sigma_g^+$ O_2 in our models is of the same nature than adsorption of $^3\Sigma_g^-$. Nevertheless, the energy gap between $^3\Sigma_g^-$ and $^1\Sigma_g^+$ decreases around 10 kJ/mol due to a stronger interaction of singlets with the zeolite framework. According to our present work, aluminosilicates reduce the triplet–singlet oxygen energy gap, showing that this system is a suitable medium for the oxidation reactions because of the expected increase of singlet oxygen population.

The interaction of O_2 with silicate and aluminosilicate clusters leads to the formation of van der Waals molecular adsorption complexes. The formation of this kind of complex is dominated by an interaction that occurs between the O atom of the non-polar molecule (O_2) and the terminal hydroxyl of the Brønsted acid site of the aluminosilicate. The weakest interaction corresponds to the oxygen molecule with the terminal silica hydroxyl groups. Singlet oxygen molecule interaction is energetically more favourable with respect to isolated molecules than the triplet oxygen molecule one. It is shown that the use of CP-corrected PES is necessary in order to obtain a good description of these very weak bonds. In such cases, BSSEs have important consequences in determining the stabilization energies. A higher basis set improves the values of the interaction energies and reduces the BSSE. Overall results are in rather good agreement with the experiment.

Consistent with AIM theory, three kinds of interactions: O–H···O, O···O, Al···O and Si–H···O appeared in the aluminosilicate–O_2 studied complexes. There are topological features of closed-shell interactions, the O–H···O appears as the most important. The larger stabilization energy of singlet complexes with respect to the triplet can be associated with the larger electron density sharing in the *bcp* relating with the O–H···O interaction.

Molecular oxygen and complexes of oxygen with other molecules have captured the attention of the theoretical and computational community and they will continue to be the focus of much research. Progress in the computational chemistry of many oxygen-related phenomena will dependent on the advances in fundamental theories and methods for the description of open-shell systems. Methods applied to these phenomena are expected in the coming years.

Acknowledgments

This work was supported by the Ministry of Higher Education (MES) of Cuba, the Deutscher Akademischer Austauschdients (DAAD) of Germany, the Universität Bremen of Germany and the Universidad Autónoma de Madrid in Spain through grants related for computer facilities. We thank W.-D. Stohrer and T. Borrmann of the Institut für Organische Chemie, Universität Bremen, Germany and Xavier Solans-Monfort of the Universitat Autònoma de Barcelona, Spain. We also thank Yamashita-Ushiyama Laboratory, University of Tokyo, Japan, for the computer facilities.

References

[1] S. Mann, G.A. Ozin, Synthesis of inorganic materials with complex form, Nature 382 (1996) 313–318.
[2] O.K. Varghese, M. Paulose, T.J. LaTempa, C.A. Grimes, High-rate solar photocatalytic conversion of CO_2 and water vapor to hydrocarbon fuels, Nano Lett. 9 (2009) 731–737.
[3] M.J. Paterson, O. Christiansen, F. Jensen, P.O. Ogilby, Overview of theoretical and computational methods applied to the oxygen-organic molecule photosystem, Photochem. Photobiol. 82 (2006) 1136–1160.
[4] H. Frei, F. Blatter, H. Sun, Photocatalyzed oxidation of hydrocarbons in zeolite cages, CHEMTECH 26 (1996) 24–30.
[5] D.M. Upadhyay, P.C. Mishra, An ab initio study of water–oxygen complexes (O_2–W_n, n = 1–6) in the ground and lowest singlet excited states, J. Mol. Struct. THEOCHEM 624 (2003) 201–224.
[6] A. Sabu, S. Kondo, R. Saito, Y. Kasai, K. Hashimoto, Theoretical study of O_2–H_2O: potential energy surface, molecular vibrations, and equilibrium constant at atmospheric temperatures, J. Phys. Chem. A 109 (2005) 1836–1842.
[7] C. Schweitzer, R. Schmidt, Physical mechanisms of generation and deactivation of singlet oxygen, Chem. Rev. 103 (2003) 1685–1758.
[8] I.V. Krylova, Electronically excited oxygen states in exoemission and heterogeneous catalytic oxidation reactions, Russ. J. Phys. Chem. A: Focus Chem. 81 (2007) 13–17.
[9] V.B. Kopylov, I.A. Yakovlev, Influence of the nature of alumina on the state of oxygen on its surface, Russ. J. Gen. Chem. 71 (2001) 639–640.
[10] E.L. Clennan, J.P. Sram, A. Pace, K. Vincer, S. White, Intrazeolite photooxidations of electron-poor alkenes, J. Org. Chem. 67 (2002) 3975–3978.

[11] E.L. Clennan, J.P. Sram, Photochemical reactions in the interior of a zeolite. Part 5. The origin of the zeolite induced regioselectivity in the singlet oxygen ene reaction, Tetrahedron Lett. 56 (2000) 6945–6950.
[12] X. Yang, B.H. Toby, M.A. Cambor, Y. Lee, D.V. Olson, Propene adsorption sites in zeolite ITQ-12: a combined synchrotron X-ray and neutron diffraction study, J. Phys. Chem. B 109 (2005) 7894–7899.
[13] M. Boronat, P.M. Viruela, A. Corma, Reaction intermediates in acid catalysis by zeolites: prediction of the relative tendency to form alkoxides or carbocations as a function of hydrocarbon nature and active site structure, J. Am. Chem. Soc. 126 (2004) 3300–3309.
[14] J. Limtrakul, T. Nanok, S. Jungsuttiwong, P. Khongpracha, T.N. Truong, Adsorption of unsaturated hydrocarbons on zeolites: the effects of the zeolite framework on adsorption properties of ethylene, Chem. Phys. Lett. 349 (2001) 161–166.
[15] L.S. Kaanumalle, J. Shailaja, R.J. Robbins, V. Ramamurthy, Cation controlled singlet oxygen mediated oxidation of olefins within zeolites, J. Photochem. Photobiol. A: Chem. 153 (2002) 55–65.
[16] H. Soscun, J. Hernández, O. Castellano, F. Arrieta, F. Ruette, A. Sierralta, F. Machado, M. Rosa-Brusin, The interaction of cis-2-butene over a 10-ring Brönsted acid site of zeolite: a theoretical study, J. Mol. Catal. A: Chem. 192 (2003) 63–72.
[17] J. Shailaja, J. Sivaguru, R.J. Robbins, V. Ramamurthy, R.B. Sunoj, J. Chandrasekhar, Singlet oxygen mediated oxidation of olefins within zeolites: selectivity and complexities, Tetrahedron 56 (2000) 6927–6943.
[18] I.V. Krylova, Electronically excited oxygen states in exoemission and heterogeneous catalytic oxidation reactions, Russ. J. Phys. Chem. A 81 (2007) 13–17.
[19] F. Wakabagashi, J.N. Kondo, K.W.a. Domer, C. Hirose, J. Phys. Chem. A 97 (1993) 10761.
[20] F. Jousse, E. Cohen de Lara, Induced infrared adsorption of molecular oxygen sorbed in exchanged A zeolites. 1. Intensity analysis, J. Phys. Chem. A 100 (1996) 238–244.
[21] D. Shen, V. Bülow, S.R. Jale, F.R. Fitch, A.F. Ojo, Thermodynamics of nitrogen and oxygen sorption on zeolites LiLSX and CaA, Micropor. Mesopor. Mater. 48 (2001) 211–217.
[22] E.M. Fernández, R.I. Eglitis, G. Borstel, L.C. Balbás, Ab initio calculations of H_2O and O_2 adsorption on Al_2O_3 substrates, Comput. Mater. Sci. 39 (2007) 587–592.
[23] M. Feuerstein, R.J. Accordi, R.F. Lobo, J. Phys. Chem. B 104 (2000) 10282.
[24] J. Plevert, L.C.d. Menorval, F.D. Renzo, F. Fajula, J. Phys. Chem. B 102 (1992) 3412.
[25] I. Salla, P. Salagre, Y. Cesteros, F.E.S.J. Medina, Study of the influence of several modernite modifications on its N_2 and O_2 adsorption properties, J. Phys. Chem. B 108 (2004) 5359–5364.
[26] H. Liu, H.-M. Kao, C.P. Grey, 1H MAS and 1H/27 Al TRAPDOR NMR studies of oxygen–zeolite interactions at low temperatures: probing Bronsted acid site accessibility, J. Phys. Chem. B 103 (1999) 4786–4796.
[27] F. Wakabayashi, T. Fujimo, J.N. Kondo, K. Domen, C. Hirose, FT-IR studies of interaction between zeolitic hydroxyl groups and small molecules. 2. Adsorption of oxygen, hydrogen, and rare gases on H-mordenite at low temperatures, J. Phys. Chem. 99 (1995) 14805–14812.
[28] F. Wakabayashi, J.N. Kondo, K. Domer, C. Hirose, FT-IR studies of the interaction between zeolitic hydroxyl groups and small molecules. 3. Adsorption of oxygen, argon, nitrogen, and xenon on H-ZSM5 at low temperatures, J. Phys. Chem. 100 (1996) 4154–4159.
[29] F. Wakabayashi, V. Kondo, K. Domnr, C. Hirose, FT-IR study of the interaction of oxygen, argon, helium, nitrogen, and xenon with hydroxyl groups in H–Y zeolite at low temperatures, Micropor. Mater. 8 (1997) 29–37.
[30] J. Sauer, P. Ugliengo, E. Garrone, V.R. Saunders, Theoretical study of van der Waals complexes at surface sites in comparison with the experiment, Chem. Rev. 94 (1994) 2095–2160.
[31] H. Mikosch, E.L. Uzunova, G.S. Nikolov, Interaction of molecular nitrogen and oxygen with extraframework cations in zeolites with double six-membered rings of oxygen-bridged silicon and aluminum atoms: a DFT study, J. Phys. Chem. B. 109 (2005) 11119–11125.
[32] E. Fois, A. Gamba, G. Tabacchi, First-principles simulation of the intracage oxidation of nitrite to nitrate sodalite, Chem. Phys. Lett. 329 (2000) 1–6.
[33] Y. Pérez-Badell, X. Solans-Monfort, M. Sodupe, L.A. Montero, DFT periodic study on the interaction between O_2 and cation exchanged chabazite MCHA (M = H^+, Na^+ or Cu^+): effects in the triplet–singlet energy gap, Phys. Chem. Chem. Phys. 12 (2010) 442–452.
[34] R.F.W. Bader, A quantum theory of molecular structure and its applications, Chem. Rev. 91 (1991) 893–928.
[35] H. Partridge, C.W. Bauschlicher, S.R. Langhoff, P.R. Taylor, Theoretical study of the low-lying bound states of O_2, J. Chem. Phys. 95 (1991) 8292–8300.
[36] K. Yamaguchi, F. Jensen, A. Dorigo, K.N. Houk, Chem. Phys. Lett. 149 (1988) 537–542.
[37] C. Møller, M.S. Plesset, Note on an approximation treatment for many-electron systems, Phys. Rev. 46 (1934) 618–622.
[38] J.M. Pérez-Jordá, A.D. Becke, A density-functional study of van der Waals forces: rare gas diatomics, Chem. Phys. Lett. 233 (1995) 134–137.
[39] R. Crespo-Otero, L.A. Montero, W.-D. Stohrer, M. Garcia de la Vega Jose, Basis set superposition error in MP2 and density-functional theory: a case of methane–nitric oxide association, J. Chem. Phys. 123 (2005) 134107.
[40] E.R. Davidson, D. Feller, Basis set selection for molecular calculations, Chem. Rev. 86 (1986) 681–696.
[41] P. Salvador, S. Simon, M. Duran, J.J. Dannenberg, J. Chem. Phys. 113 (2000) 5666–5674.
[42] S.F. Boys, F. Bernardi, The calculation of small molecular interactions by the differences of separate total energies. Some procedures with reduced errors, Mol. Phys. 19 (1970) 553–566.
[43] M.W. Wong, M.J. Frisch, K.B. Wiberg, Solvent effects. 1. The mediation of electrostatic effects by solvents, J. Am. Chem. Soc. 113 (1991) 4776–4782.
[44] B. Mennucci, J. Tomasi, Continuum solvation models. A new approach to the problem of solute's distribution and cavity boundaries, J. Chem. Phys. 106 (1997) 5151–5158.
[45] M.J. Frisch, G.W. Trucks, H.B. Schlegel, G.E. Scuseria, M.A. Robb, J.R. Cheeseman, V.G. Zakrzewski, J.A. Montgomery Jr., R.E. Stratmann, J.C. Burant, S. Dapprich, J.M. Millam, A.D. Daniels, K.N. Kudin, M.C. Strain, O. Farkas, J. Tomasi, V. Barone, M. Cossi, R. Cammi, B. Mennucci, C. Pomelli, C. Adamo, S. Clifford, J. Ochterski, G.A. Petersson, P.Y. Ayala, Q. Cui, K. Morokuma, D.K. Malick, A.D. Rabuck, K. Raghavachari, J.B. Foresman, J. Cioslowski, J.V. Ortiz, A.G. Baboul, B.B. Stefanov, G. Liu, A. Liashenko, P. Piskorz, I. Komaromi, R. Gomperts, R.L. Martin, D.J. Fox, T. Keith, M.A. Al-Laham, C.Y. Peng, A. Nanayakkara, C. Gonzalez, M. Challacombe, P.M.W. Gill, B. Johnson, W. Chen, M.W. Wong, J.L. Andres, C. Gonzalez, M. Head-Gordon, E.S. Replogle, J.A. Pople, Gaussian 98, Revision A.7, Gaussian, Inc., Pittsburgh, 1998.
[46] M.J. Frisch, G.W. Trucks, H.B. Schlegel, G.E. Scuseria, M.A. Robb, J.R. Cheeseman, J.A. Montgomery Jr., T. Vreven, K.N. Kudin, J.C. Burant, J.M. Millam, S.S. Iyengar, J. Tomasi, V. Barone, B. Mennucci, M. Cossi, G. Scalmani, N. Rega, G.A. Petersson, H. Nakatsuji, M. Hada, M. Ehara, K. Toyota, R. Fukuda, J. Hasegawa, M. Ishida, T. Nakajima, Y. Honda, O. Kitao, H. Nakai, M. Klene, X. Li, J.E. Knox, H.P. Hratchian, J.B. Cross, C. Adamo, J. Jaramillo, R. Gomperts, R.E. Stratmann, O. Yazyev, A.J. Austin, R. Cammi, C. Pomelli, J.W. Ochterski, P.Y. Ayala, K. Morokuma, G.A. Voth, P. Salvador, J.J. Dannenberg, V.G. Zakrzewski, S. Dapprich, A.D. Daniels, M.C. Strain, O. Farkas, D.K. Malick, A.D. Rabuck, K. Raghavachari, J.B. Foresman, J.V. Ortiz, Q. Cui, A.G. Baboul, S. Clifford, J. Cioslowski, B.B. Stefanov, G. Liu, A. Liashenko, P. Piskorz, I. Komaromi, R.L. Martin, D.J. Fox, T. Keith, M.A. Al-Laham, C.Y. Peng, A. Nanayakkara, M. Challacombe, P.M.W. Gill, B. Johnson, W. Chen, M.W. Wong, C. Gonzalez, J.A. Pople, Gaussian 03, Gaussian, Inc., Pittsburgh, 2003.
[47] L.J. Farrugia, ORTEP-3 for Windows—a version of ORTEP-III with a graphical user interface (GUI), J. Appl. Cryst. 30 (1997) 565.
[48] J. Beckmann, S. Grabowsky, Supramolecular silanol chemistry in the gas phase. Topological (AIM) and population (NBO) analyses of hydrogen-bonded complexes between H_3SiOH and selected O- and N-acceptor molecules, J. Phys. Chem. A 111 (2007) 2011–2019.
[49] M.F. Salazar, N.M. Peruchena, Topological analysis of the electronic charge density in the ethene protonation reaction catalyzed by acidic zeolite, J. Phys. Chem. A 111 (2007) 7848–7859.
[50] G.V. Gibbs, D. Jayatilaka, M.A. Spackman, D.F. Cox, K.M. Rosso, Si–O bonded interactions in silicate crystals and molecules: a comparison, J. Phys. Chem. A 110 (2006) 12678–12683.
[51] A. Kyrlidis, S.J. Cook, A.K. Chakraborty, A.T. Bell, D.N. Theodorou, Electronic structure calculations of ammonia adsorption in H-ZSM-5 zeolites, J. Phys. Chem. 99 (1995) 1505–1515.
[52] G.J. Kramer, A.J.M. de Man, R.A. van Santen, Zeolites versus aluminosilicate clusters: the validity of a local description, J. Am. Chem. Soc. 133 (1991) 6435.
[53] N.B. Okulik, R.P. Diez, A.H. Jubert, Topological study of the effect of the isomorphic substitution of silicon by aluminum on the zeolite structure and its interaction with methane, J. Phys. Chem. A 107 (2003) 6225–6230.
[54] F.B. Konig, J. Schonbohm, D.J. Bayles, Comput. Chem. 22 (2001) 545.
[55] S. Simon, M. Duran, J.J.J. Dannenberg, Chem. Phys. 105 (1996) 11024.
[56] R.F.W. Bader; Atoms in Molecules: A Quantum Theory; Oxford University Press: Oxford, U.K., 1990.
[57] S. Jenkins, I. Morrison, The chemical character of the intermolecular bonds of seven phases of ice as revealed by ab initio calculation of electron densities, Chem. Phys. Lett. 317 (2000) 97–102.